Developmental Cell
Article

Cyclin E Constrains Cdk5 Activity to Regulate Synaptic Plasticity and Memory Formation

Junko Odajima,[1,3,8] Zachary P. Wills,[4,8,9] Yasmine M. Ndassa,[1,5] Miho Terunuma,[6] Karla Kretschmannova,[6] Tarek Z. Deeb,[6] Yan Geng,[1,3] Sylwia Gawrzak,[1,3] Isabel M. Quadros,[6] Jennifer Newman,[6] Manjusri Das,[1] Marie E. Jecrois,[1,3] Qunyan Yu,[1] Na Li,[1,3] Frederic Bienvenu,[1,10] Stephen J. Moss,[6,7] Michael E. Greenberg,[4] Jarrod A. Marto,[1,2,5,*] and Piotr Sicinski[1,3,*]
[1]Department of Cancer Biology
[2]Blais Proteomics Center
Dana-Farber Cancer Institute, Boston, MA 02215, USA
[3]Department of Genetics
[4]Department of Neurobiology
[5]Department of Biological Chemistry and Molecular Pharmacology and Biophysics Program
Harvard Medical School, Boston, MA 02115, USA
[6]Center for Neuroscience Research, Department of Neuroscience, Tufts University School of Medicine, Boston, MA 02111, USA
[7]Department of Neuroscience, Physiology and Pharmacology, University College, London WC1E 6BT, UK
[8]These authors contributed equally to this work
[9]Present address: Department of Neurobiology, University of Pittsburgh, Pittsburgh, PA 15213, USA
[10]Present address: Institute of Functional Genomics, UMR 5203 CNRS, U 661 INSERM, Universite de Montpellier, 34094 Montpellier, France
*Correspondence: jarrod_marto@dfci.harvard.edu (J.A.M.), peter_sicinski@dfci.harvard.edu (P.S.)
DOI 10.1016/j.devcel.2011.08.009

SUMMARY

Cyclin E is a component of the core cell cycle machinery, and it drives cell proliferation by regulating entry and progression of cells through the DNA synthesis phase. Cyclin E expression is normally restricted to proliferating cells. However, high levels of cyclin E are expressed in the adult brain. The function of cyclin E in quiescent, postmitotic nervous system remains unknown. Here we use a combination of in vivo quantitative proteomics and analyses of *cyclin E* knockout mice to demonstrate that in terminally differentiated neurons cyclin E forms complexes with Cdk5 and controls synapse function by restraining Cdk5 activity. Ablation of cyclin E led to a decreased number of synapses, reduced number and volume of dendritic spines, and resulted in impaired synaptic plasticity and memory formation in cyclin E-deficient animals. These results reveal a cell cycle-independent role for a core cell cycle protein, cyclin E, in synapse function and memory.

INTRODUCTION

The mammalian core cell cycle machinery is composed of cyclins and their associated cyclin-dependent kinases (Cdks). Cyclin-Cdk complexes phosphorylate cellular proteins, thereby driving cell cycle progression (Malumbres and Barbacid, 2009).

Cyclins are induced in a coordinated fashion to enable cell proliferation. Thus, in response to growth factor stimulation D-type cyclins (D1, D2, and D3) are upregulated and subsequently bind and activate Cdk4 and Cdk6. Cyclin D-Cdk4/6 kinase phosphorylates the retinoblastoma protein, pRB, leading to the release or derepression of E2F transcription factors and to transcriptional induction of the E-type cyclins (cyclins E1 and E2) (Sherr and Roberts, 2004). The two E-cyclins share significant amino acid identity, are coexpressed in all proliferating cell types, and appear to have entirely overlapping functions (Geng et al., 2001; Gudas et al., 1999; Koff et al., 1991; Lauper et al., 1998; Lew et al., 1991; Zariwala et al., 1998).

Cyclin E affects cell proliferation by multiple mechanisms. Once induced in late G1 phase, E-cyclins bind and activate Cdk2 and Cdk1 and further phosphorylate pRB. In addition, cyclin E-Cdk holoenzyme phosphorylates proteins involved in initiation of DNA replication, proteins governing centrosome duplication, histone biosynthesis, and cell cycle progression. All these functions contribute to the well-established role for cyclin E in cell proliferation (Hwang and Clurman, 2005).

Consistent with their growth-promoting functions, overexpression of cyclins E1 and E2 is seen in a substantial fraction of human cancers, including mammary carcinomas, lung, endometrial, gastric, colorectal, and ovarian cancers, as well as sarcomas, lymphomas, and leukemias. In several cancer types overexpression of cyclin E was shown to confer poor prognosis (Hwang and Clurman, 2005).

In the past, we and others studied the functions of cyclin E in development by generating *cyclin E* knockout mice. Cyclin E deficient ($E1^{-/-}E2^{-/-}$) mice died early during gestation due to placental abnormalities (Geng et al., 2003; Parisi et al., 2003). In addition, cyclin E was required for normal heart development and for cell cycle re-entry of embryonic fibroblasts (Geng et al., 2003). All these findings were consistent with the role for cyclin E in cell proliferation.

Expression of cyclin E is usually limited to proliferating cells. Consequently, quiescent organs of adult mice express very little or no cyclin E protein. An exception to this rule is provided by the observations that cyclin E is expressed at high levels

in the brains of adult mice (Geng et al., 2001; Ikeda et al., 2011; Miyajima et al., 1995). However, the function of cyclin E in nonproliferating brain cells remained unknown.

In this study, we provide evidence that in terminally differentiated neurons cyclin E regulates formation of synapses, by inhibiting Cdk5, an essential regulator of neuronal differentiation. These findings reveal an unexpected function of a core cell cycle protein in postmitotic neurons, and may have implications for our understanding of neurological disorders, such as Alzheimer disease, in which Cdk5 disregulation has been implicated as a causative factor (Cruz and Tsai, 2004).

RESULTS

Cyclin E Expression in Adult Brain

We started our analyses by verifying that brains of adult mice express high levels of cyclin E. This was in contrast to other adult organs composed of nonproliferating cells, which expressed very little cyclin E (Figure 1A). We observed that the levels of cyclin E in brains of adult mice were similar to those seen in embryonic brains, the latter containing a high proportion of proliferating neuronal progenitors (Figure 1A). Developmental analysis revealed that in brains, cyclin E levels peak during embryonic development, decline at birth, and then increase again during postnatal life when much of neuronal differentiation takes place (Figure 1B). In adult brains, cyclin E is expressed in most anatomical regions, including cerebral cortex and hippocampus (Figure 1C). Coimmunostaining of adult brain sections for cyclin E and neuronal-specific marker NeuN revealed that cyclin E is expressed in terminally differentiated neurons, but not in glial cells (Figure 1D; see Figures S1A and S1B available online). Subcellular fractionation of adult brain cortices demonstrated that cyclin E is present predominantly in the cytoplasm, and to a lesser extent in the nucleus (data not shown). Consistent with these findings, immunofluorescence studies of cultured primary neurons revealed that cyclin E is localized in the cell soma, and enriched in dendrites as well as in axons (Figure 1E, Figure S1C, and data not shown). These observations are in contrast to dividing cells, where cyclin E is largely nuclear (Hwang and Clurman, 2005; Ohtsubo et al., 1995), suggesting that in postmitotic neurons cyclin E may function in a manner distinct from its role in the cell cycle.

Quantitative Proteomic Analyses of Adult Mouse Brain

To gain molecular insights into cyclin E function in the brains of adult animals, we generated a knock-in mouse strain expressing Flag- and hemagglutinin (HA)-tandemly tagged version of cyclin E1. We reasoned that these mice would allow us to use sequential immunoaffinity purifications with anti-Flag and -HA antibodies, followed by quantitative mass spectrometry, to compare the set of cyclin E1-interacting proteins in adult versus in embryonic brains.

To generate tagged knock-in mice, DNA sequences encoding Flag- and HA-tags were inserted into the amino-terminus of the endogenous *cyclin E1* locus through gene targeting in embryonic stem cells (Figure 2A). Once homozygous mice were obtained, we verified that in the tissues of knock-in mice the expression pattern and function of the tagged cyclin E1 faithfully mirrored those of the endogenous cyclin E1 in wild-type animals (Figures S2A–S2D and data not shown).

We then purified cyclin E1-associated protein complexes from adult and embryonic brains using sequential immunoaffinity purifications with anti-Flag and -HA antibodies (Figure S2E) and performed protein identification using high-sensitivity nanoflow liquid chromatography tandem mass spectrometry (LC-MS/MS) (Table S1). To obtain a quantitative measure of the differences between the sets of cyclin E1-interacting proteins in adult versus embryonic brains, we used iTRAQ reagents (Ross et al., 2004) in a quantitative mass spectrometry approach. Briefly, proteins present in purification products from adult and embryonic brains were separately labeled with distinct iTRAQ stable isotope reagents. Subsequently, the samples were mixed and subjected to quantitative LC-MS/MS analysis.

We found that known cell cycle partners of cyclin E1, such as Cdk1 and Cdk2, were enriched among cyclin E1-containing complexes in embryonic brains (Figures 2B and 2C and Table S2), consistent with cell cycle-promoting function of cyclin E in proliferating cells. Surprisingly, in adult brains we found that Cdk5, a Cdk-related protein that regulates neuronal differentiation (Dhavan and Tsai, 2001), was strongly enriched in cyclin E1-containing complexes (Figures 2B and 2C and Table S2). We verified abundant association of cyclin E1 with Cdk5 in adult, but not in embryonic brains by immunoprecipitation western blotting (Figures 3A and 3B). We estimated using immunodepletion analyses that virtually all cyclin E1 molecules are bound to Cdk5 in adult brains (Figure 3C).

Consistent with these findings, developmental analyses revealed that embryonic brains express cyclin E and Cdk2, but very little Cdk5. Upon birth, the expression of Cdk2 is extinguished, whereas the levels of Cdk5 become upregulated, concomitant with induction of cyclin E (Figure 1B).

In addition to Cdk5, $p27^{Kip1}$, an inhibitor of cyclin-dependent kinases, was enriched among cyclin E1-binding proteins in adult brain (Figures 2B and 2C and Table S2), suggesting a possibility of a ternary cyclin E1-Cdk5-$p27^{Kip1}$ complex. We determined by sequential immunoprecipitations that cyclin E1, Cdk5, and $p27^{Kip1}$ indeed form a ternary complex in adult mouse brain (Figure S3A).

Cyclin E-Cdk5 Complex Is Catalytically Inactive and Is Induced During Synaptogenesis

Cdk5 is expressed in nonproliferating, postmitotic neurons in the nervous tissue, where it binds and becomes catalytically activated by its regulatory partners, p35 and p39 (Lew et al., 1994; Tsai et al., 1993, 1994). These p35/p39-Cdk5 complexes control many aspects of neuronal differentiation by phosphorylating several neuronal substrates (Dhavan and Tsai, 2001). It was previously shown, based on the crystal structure of p25- (a fragment of p35) Cdk5 complex, that p35/p39 regulates Cdk5 via a mechanism that is distinct from the one used by cyclins to activate Cdk2 (Tarricone et al., 2001). This, together with the presence of a Cdk-inhibitor $p27^{Kip1}$ in ternary complexes with cyclin E1-Cdk5 (Figure S3A) suggested that Cdk5 would be catalytically inactive in these complexes. We tested this prediction by in vitro kinase assays, and found that cyclin E1-Cdk5 was unable to phosphorylate several known Cdk5 substrates (Figure 3D and Figure S3B). These results suggested that cyclin E may prevent

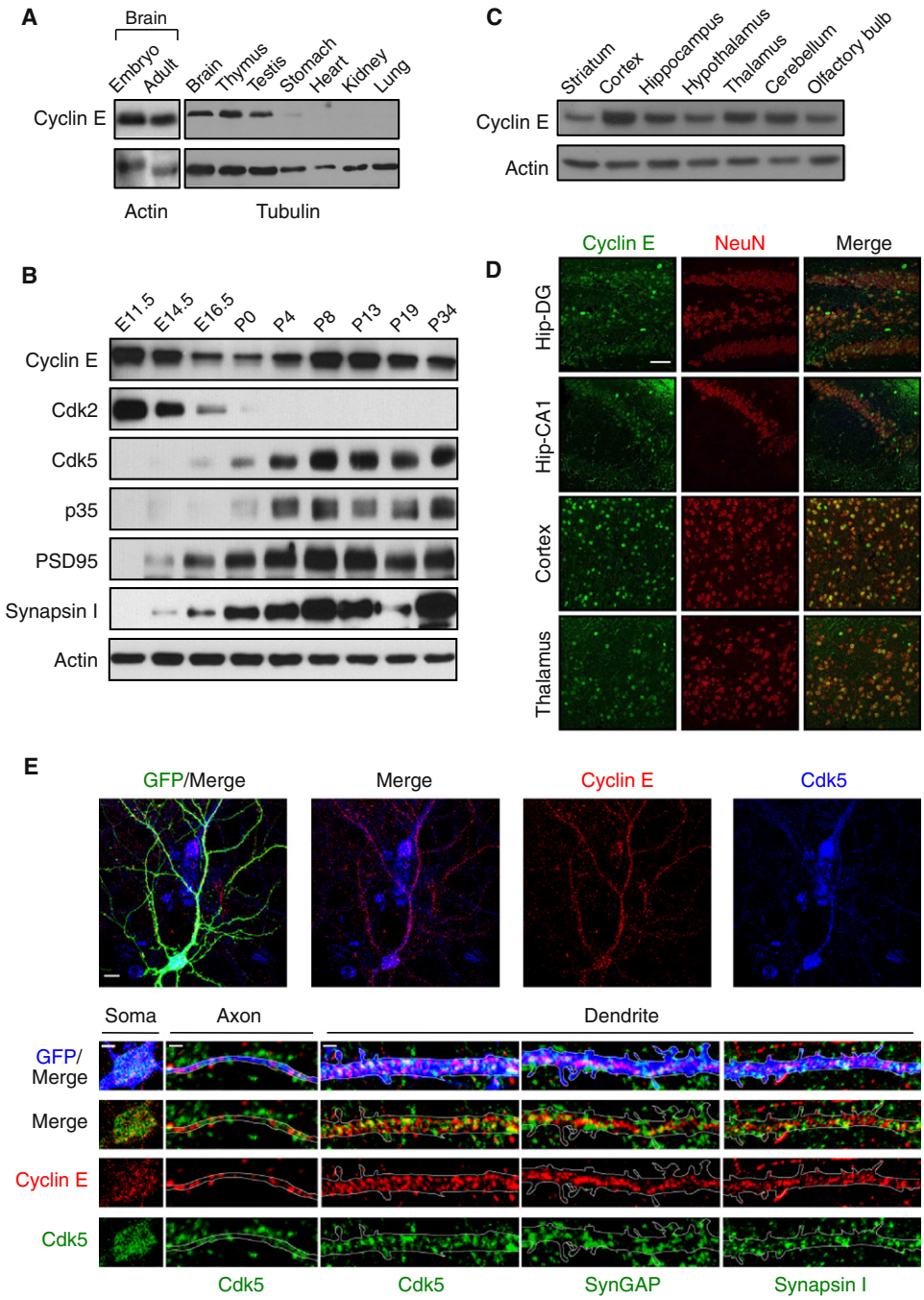

Figure 1. Cyclin E Expression in Postmitotic Neurons

(A) Cyclin E levels were detected by western blotting in the indicated organs of adult mice and in embryonic brain.

(B) Western blot analysis of frontal brain (for E11.5 and E14.5) and cortices dissected from mice at the indicated days of embryonic (E) or postnatal (P) development. Immunoblots were probed with antibodies against the indicated cell cycle and synaptic proteins.

(C) Western blot analysis of cyclin E levels in the indicated structures of adult mouse brain.

(D) Cyclin E and NeuN immunostaining in adult mouse brain. Hip-DG, hippocampus, dentate gyrus; Hip-CA1, hippocampal CA1 region. Scale bar represents 25 μm.

(E) Sixteen-day in vitro cultured hippocampal neurons were transfected with GFP, and stained with the indicated antibodies. Scale bars represent 10 μm in top panel, 5 μm in soma images, and 1 μm in axon and dendrite images. SynGAP and Synapsin I were used as post- and presynaptic markers, respectively. See also Figure S1.

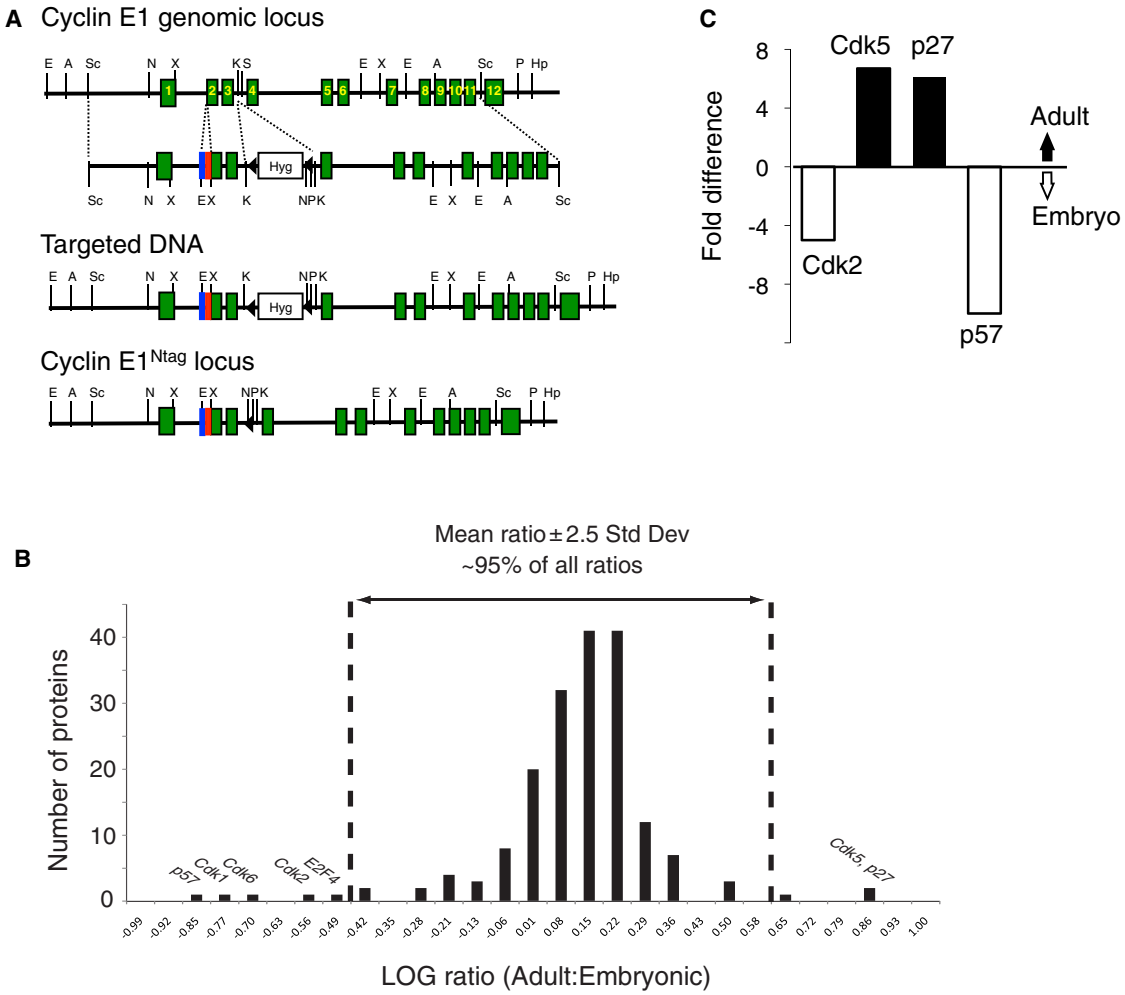

Figure 2. In Vivo Quantitative Proteomic Analyses

(A) Gene-targeting strategy to generate tagged cyclin E knock-in mice. Sequences encoding Flag- and HA-tags (blue and red box, respectively) were inserted at the amino terminus of cyclin E1.

(B) Histogram of iTRAQ log ratios. Ratios for peptides identified in quantitative LC-MS/MS analyses were combined to give corresponding protein ratios representing the relative abundance of cyclin E1 protein interactors for adult versus embryonic brain. The LOG_{10} of these ratios was then plotted as a histogram distribution. Protein ratios that fell outside ±2.5 standard deviations (0.533) relative to the mean LOG ratio for all proteins (0.078) constituted the set of the ~5% most extreme ratios, and thus were considered enriched in adult or embryonic brains, respectively, as cyclin E-interacting proteins (see Table S2). Cdk1, Cdk2, Cdk6, $p57^{Kip2}$, and E2F4 were found enriched in embryonic brains, and Cdk5 and $p27^{Kip1}$ in adult brains.

(C) Shown is fold-enrichment of the indicated proteins within cyclin E-containing complexes in adult versus in embryonic brain samples, as detected by the iTRAQ analysis.

See also Figure S2.

Cdk5 activation by recruiting it into catalytically inactive complexes, and by sequestering it away from p35/p39, the only known Cdk5 activator. To test this hypothesis, we overexpressed increasing amounts of cyclin E1 along with constant levels of Cdk5 and p35 in heterologous cells. Consistent with our hypothesis, these analyses revealed that cyclin E1 can compete with p35 for Cdk5 binding (Figures 3F and 3G).

In order to further investigate the function of cyclin E-Cdk5 in neurons, we isolated mouse embryonic hippocampal neurons and cultured them in vitro. We found that expression of cell cycle proteins, such as cyclin A and Cdk2 declined as cells matured. In contrast, cyclin E and Cdk5 became induced in the course of neuronal differentiation (Figure 3E). Furthermore, the induction of cyclin E and Cdk5 in hippocampal neurons coincided with the induction of synaptic proteins and with the onset of synaptogenesis (Figure 3E and data not shown). We noted a similar correlation in vivo, during postnatal brain development (Figure 1B). Because Cdk5 was shown to play an important role in synapse formation and synaptic plasticity (Dhavan and Tsai, 2001), our findings suggested the possibility that cyclin E might influence Cdk5 function in these processes.

Decreased Numbers of Synapses in Cyclin E-Deficient Neurons

To analyze the function of cyclin E in synapse physiology, we generated a *cyclin* $E1^{flox/flox}$ mouse strain (Figure S4A). We

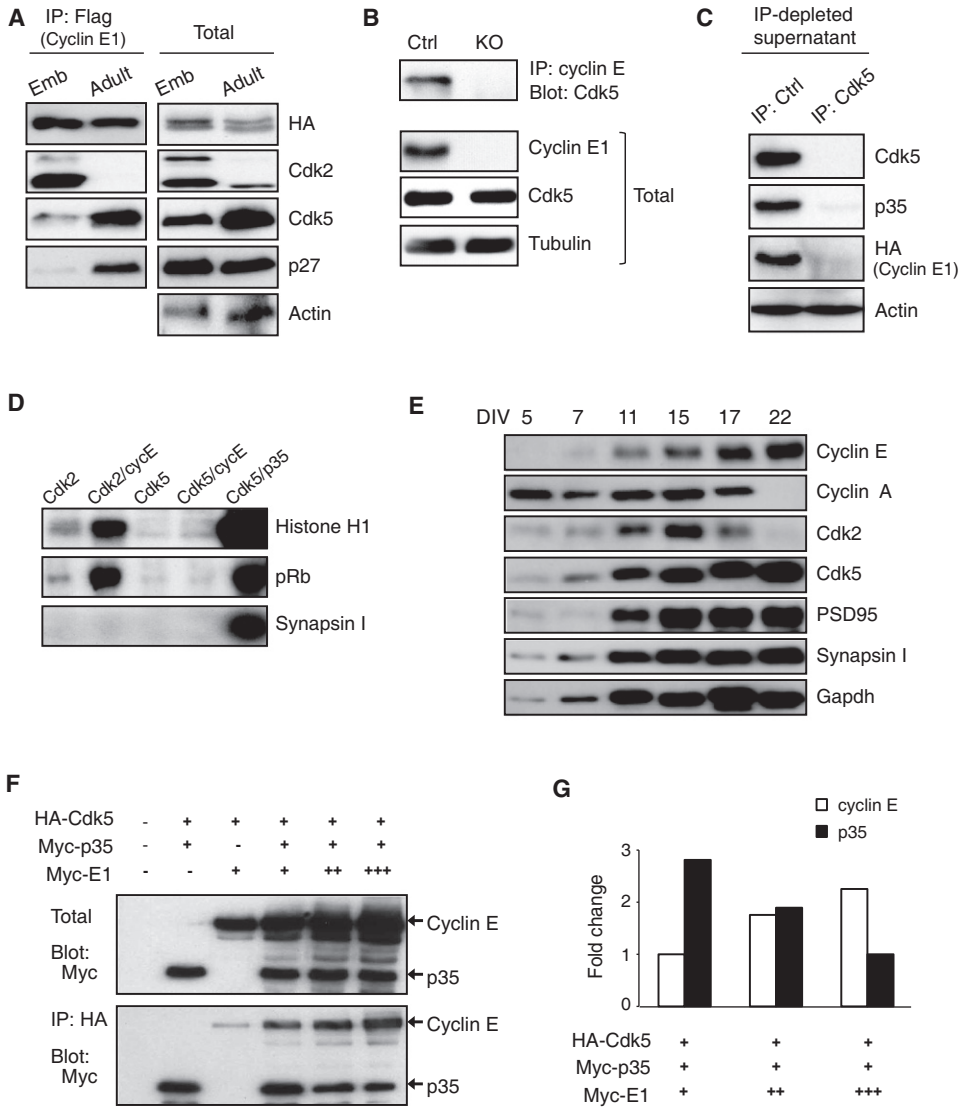

Figure 3. Analyses of Cyclin E-Cdk5 Complex

(A) Cyclin E was immunoprecipitated with anti-Flag antibody from embryonic and adult brains of *cyclin E1*$^{Ntag/Ntag}$ mice, and immunoblots were probed with the indicated antibodies. Total lysates were also analyzed.

(B) Endogenous cyclin E was immunoprecipitated from brains of adult wild-type mice (Ctrl) or from brains of conditional *cyclin E* knockout-*Nestin-Cre* animals (KO) as a negative control, and the immunoblots were probed for Cdk5. Total levels of cyclin E1 and Cdk5 in protein lysates are also shown.

(C) Immunodepletioin anaysis to quantify cyclin E1-Cdk5 interaction. Brain lysates were prepared from adult *cyclin E1*$^{Ntag/Ntag}$ knock-in mice and subjected to two rounds of immunodepletion with IgG (IP: Ctrl) or anti-Cdk5 antibodies (IP: Cdk5). Depletion of the indicated proteins was analyzed by probing the supernatants with the indicated antibodies.

(D) 293T cells were transfected with HA-tagged Cdk2 or Cdk5 alone, or together with Myc-tagged cyclin E1 or p35. Cell lysates were immunoprecipitated with anti-HA antibody and in vitro kinase reactions were performed with purified Cdk5 substrates: histone H1, retinoblastoma protein (pRb), or Synapsin I. Note that cyclin E-Cdk5 complexes were unable to phosphorylate these substrates, in contrast to p35-Cdk5 complexes, which served as a positive control. Importantly, cyclin E-Cdk2 can phosphorylate its substrates: histone H1 and pRb.

(E) Dissociated hippocampal neuronal cultures were analyzed by immunoblotting at the indicated days postplating (days in vitro, DIV) with the indicated antibodies, including anti-PSD95 (postsynaptic marker), and anti-Synapsin I (presynaptic marker).

(F) 293T cells were cotransfected with constant amounts of plasmids encoding HA-tagged Cdk5 and Myc-tagged p35 together with increasing amounts of Myc-tagged cyclin E1. Upper panel: the levels of ectopically expressed cyclin E and p35 were determined by probing immunoblots with anti-Myc antibody. Lower panel: association of Cdk5 with cyclin E and with p35 was assessed by immunoprecipitating Cdk5 with anti-HA antibody followed by immunoblotting with anti-Myc antibody.

(G) Quantification of the amounts of cyclin E and p35 coimmunoprecipitating with Cdk5, corresponding to the lanes 4–6 of the lower panel in (F).

See also Figure S3.

next interbred *cyclin E1*$^{flox/flox}$ and *cyclin E2*$^{-/-}$ animals, and obtained *cyclin E1*$^{flox/flox}$*E2*$^{-/-}$ mice (Figure S4B).

We started our analyses by dissecting hippocampi from these mice and by establishing in vitro cultures of dissociated hippocampal neurons. Ten days after plating, postmitotic neurons were transfected with GFP and Cre. Subsequently, synapse formation was assessed by staining the cultures for the presynaptic marker Synapsin I and excitatory postsynaptic marker PSD95, and the number of colocalized Synapsin I and PSD95 puncta on transfected neurons was quantified. Strikingly, acute deletion of cyclin E in postmitotic neurons resulted in a significant decrease of PSD95/Synapsin I puncta (Figures 4A and 4B and Figure S4D), indicating a reduced number of excitatory synapses. We extended these observations by measuring spontaneous miniature excitatory postsynaptic currents (mEPSC) in cultured cyclin E-deficient neurons. mEPSCs gauge the strength and number of synaptic inputs onto a recorded neuron. We found that an acute ablation of cyclin E led to a significant decrease of mEPSC amplitudes and frequency (Figures 4C and 4D and Figure S4E), which is indicative of reduced synapse number and reduced synaptic transmission. Collectively these results revealed a significant decrease in the number and function of excitatory synapses following an acute ablation of cyclin E in postmitotic neurons.

Decreased Numbers of Dendritic Spines in *Cyclin E* Null Neurons

To further substantiate these findings, we analyzed the impact of cyclin E ablation within the context of an intact neuronal circuit. To this end, we prepared hippocampal slices from *cyclin E1*$^{flox/flox}$*E2*$^{-/-}$ mice. We biolistically transfected the slices with Cre and GFP, and quantified the number of dendritic spines, which represent postsynaptic sites of excitatory synapses in the brain, in GFP-positive CA1 hippocampal pyramidal neurons. Consistent with our previous findings, we observed reduced numbers of dendritic spines upon acute cyclin E shutdown in all dendritic regions of CA1 hippocampal neurons (proximal, distal, and basal) (Figures 4E and 4F).

Collectively, our analyses of cyclin E-deficient neurons and hippocampal slices indicated that cyclin E promotes the establishment of dendritic spines and the formation of functional synapses. We next investigated a possible mechanism by which cyclin E might affect these processes.

Mechanistic Analyses of Cyclin E-Cdk5 Synaptic Function

Based on our observations that cyclin E-Cdk5 complexes are catalytically inactive (Figure 3D), and that cyclin E can compete with p35 for Cdk5 binding (Figures 3F and 3G), we hypothesized that cyclin E serves to sequester Cdk5 away from its activators p35 and p39, into inactive cyclin E-Cdk5 complexes. We further hypothesized that ablation of cyclin E and the loss of inhibitory cyclin E-Cdk5 complexes results in hyperactivation of Cdk5, leading to the observed reduction in synapse number. This hypothesis was consistent with several reports that Cdk5 can play an inhibitory role in synapse formation and function (Chergui et al., 2004; Kim et al., 2006; Kim and Ryan, 2010; Morabito et al., 2004).

We tested this model first by overexpressing Cdk5 in in vitro cultured control neurons. We found that Cdk5 overexpression indeed phenocopied cyclin E ablation, namely it reduced the numbers of excitatory synapses (Figures 4A and 4B). Moreover, we found that knock-down of Cdk5 (Figure S1D), or expression of dominant-negative Cdk5 mutant (Nikolic et al., 1996) reversed the synaptic deficits in cyclin E null neurons (Figures 4A and 4B). Lastly, we observed that knock-down of Cdk5 in organotypic hippocampal slices restored normal numbers of dendritic spines in cyclin E-deficient neurons (Figure 4G). All these observations were consistent with the notion that cyclin E constrains Cdk5 activity and that hyperactivation of Cdk5 leads to synaptic phenotypes in *cyclin E* null neurons.

Molecular Analyses of Brains from Conditional *Cyclin E* Knockout Mice

A direct test of the model proposed above would be to determine the phosphorylation status of synaptic Cdk5 substrates on Cdk5-specific residues in the brains of *cyclin E* null mice. To accomplish this, we interbred *cyclin E1*$^{flox/flox}$*E2*$^{-/-}$ mice with *Nestin-Cre* animals, which constitutively express Cre recombinase in the nervous system (Tronche et al., 1999), and verified efficient deletion of cyclin E in the brains of cyclin E knockout-*Nestin-Cre* mice (Figures S4B and S4C). Because in *Nestin-Cre* mice, expression of Cre is turned on in proliferating embryonic neuronal progenitors (Graus-Porta et al., 2001), ablation of cyclin E in embryogenesis might have affected brain development. However, we established that ablation of cyclin E did not affect proliferation rates throughout embryonic brain development (Figure S5A). Also, the number of nestin-positive neural stem/progenitor cells was unperturbed in *cyclin E* null fetal brains (Figure S5B). Adult cyclin E-deficient brains displayed normal anatomical structures (Figures S5C–S5E) and normal staining with a panel of neuronal and glial cell markers such as Ctip2, Cux1, GABA, calbindin, parvalbumin, Olig2, and GFAP (Figures S1A and S1B and data not shown). Moreover, normal numbers of proliferating progenitor cells were seen in the subventricular zone of adult cyclin E-deficient brains (data not shown). Hence, ablation of cyclin E in the nervous system did not adversely affect proliferation rates and development of the brain, as we have previously shown to be the case with most other organs in cyclin E-deficient embryos (Geng et al., 2003).

We then dissected hippocampi and cerebral cortices from adult *cyclin E* knockout-*Nestin-Cre* mice and analyzed the phosphorylation status of Wave1 (Kim et al., 2006) and Synapsin I (Matsubara et al., 1996), two known synaptic Cdk5 targets, using antibodies directed against Cdk5-specific phosphoresidues on these proteins (Ser553 on Synapsin I, Ser310 and Ser441 on Wave1). Consistent with our hypothesis of Cdk5 hyperactivation, we observed increased phosphorylation of these residues in cyclin E-deficient hippocampi as well as in cortices (Figures 5A and 5B). In addition, increased phosphorylation of Cdk5 substrates was also seen in in vitro cultured hippocampal neurons from *cyclin E* knockout-*Nestin-Cre* mice (data not shown). Importantly, acute ablation of cyclin E in in vitro cultured postmitotic neurons led to increased phosphorylation of Wave1, whereas knock-down of Cdk5 reversed this effect (Figures 5C and 5D), confirming that hyperactivation of Cdk5 is also seen upon acute deletion of cyclin E. Phosphorylation of Wave1 on

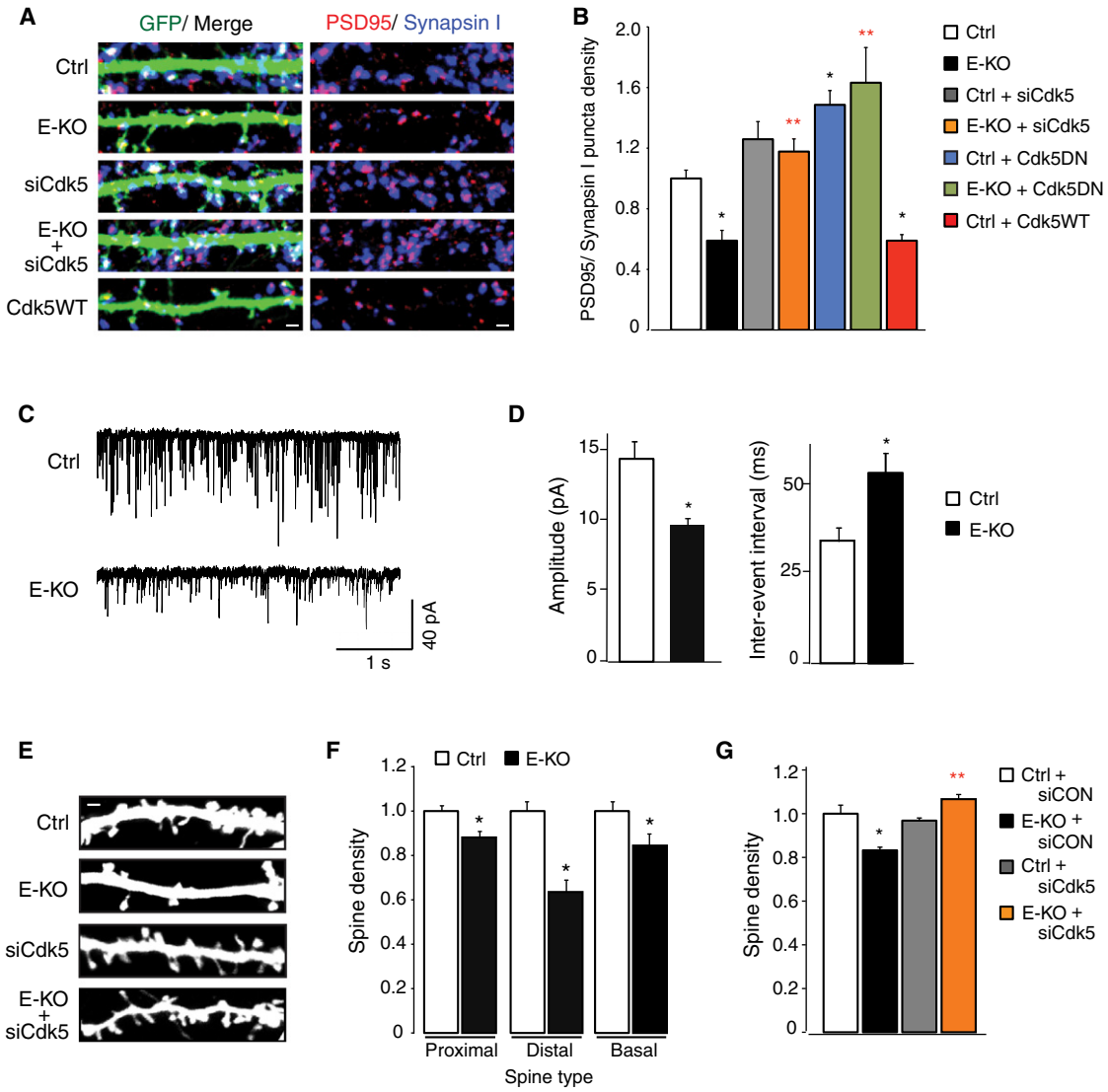

Figure 4. Reduced Synapse Numbers in *Cyclin E* Null Neurons

(A) Images of GFP-transfected *cyclin E1*$^{flox/flox}$*E2*$^{+/-}$ (Ctrl), or GFP- and Cre-transfected *cyclin E1*$^{flox/flox}$*E2*$^{-/-}$ (E-KO) hippocampal neurons stained for Synapsin I and PSD95. Scale bars represent 2 μm.

(B) Quantification of the density of colocalized PSD95/Synapsin I puncta in Ctrl and E-KO hippocampal neurons. In the indicated experiments, neurons were also transfected with Cdk5 siRNA (siCdk5), a wild-type Cdk5 expression construct (Cdk5WT), or a dominant negative Cdk5 expression construct (Cdk5DN). Transfection of control siRNA did not show any significant difference relative to control (data not shown). Data are normalized to GFP-transfected control and represent mean ± SEM from three to five independent experiments; total numbers of neurons analyzed, n = 30 to 60 cells/condition. *p < 0.05 versus Ctrl; red **p < 0.05 versus E-KO; one-way ANOVA with pairwise comparison by Tukey's post hoc test.

(C) Representative mEPSC recorded from GFP-transfected *cyclin E1*$^{flox/flox}$*E2*$^{+/-}$ (Ctrl) and GFP- and Cre-transfected *cyclin E1*$^{flox/flox}$*E2*$^{-/-}$ (E-KO) primary hippocampal neurons.

(D) Mean amplitudes and mean inter-event intervals of mEPSC recordings of Ctrl and E-KO neurons. *p < 0.05; Student's t test. The graphs represent mean values ± SEM; n = 8 for Ctrl and n = 8 for E-KO neurons.

(E) Representative images of dendritic spines, visualized by immunostaining with anti-GFP antibody. Scale bar represents 2 μm.

(F) Normalized quantification of dendritic spine density in Ctrl and E-KO CA1 hippocampal pyramidal neurons. Hippocampal slices from Ctrl and E-KO mice were biolistically transfected with GFP or Cre plus GFP, respectively, and analyzed after 5 days. *p < 0.05; Student's t test. Shown are means ± SEM from three independent experiments; n = 25–50 cells/condition.

(G) Normalized quantification of dendritic spine density (proximal, distal, and basal densities combined) following biolistic transfection of control siRNA (siCON) or Cdk5 siRNA (siCdk5) in combination with either GFP alone (Ctrl) or GFP plus CRE (E-KO). *p < 0.05 versus Ctrl + siCON; red **p < 0.05 versus E-KO + siCON; one-way ANOVA with pairwise comparison by Bonferroni post hoc test. Shown are means ± SEM from three independent experiments; n = 60–80 cells/condition. See also Figure S4.

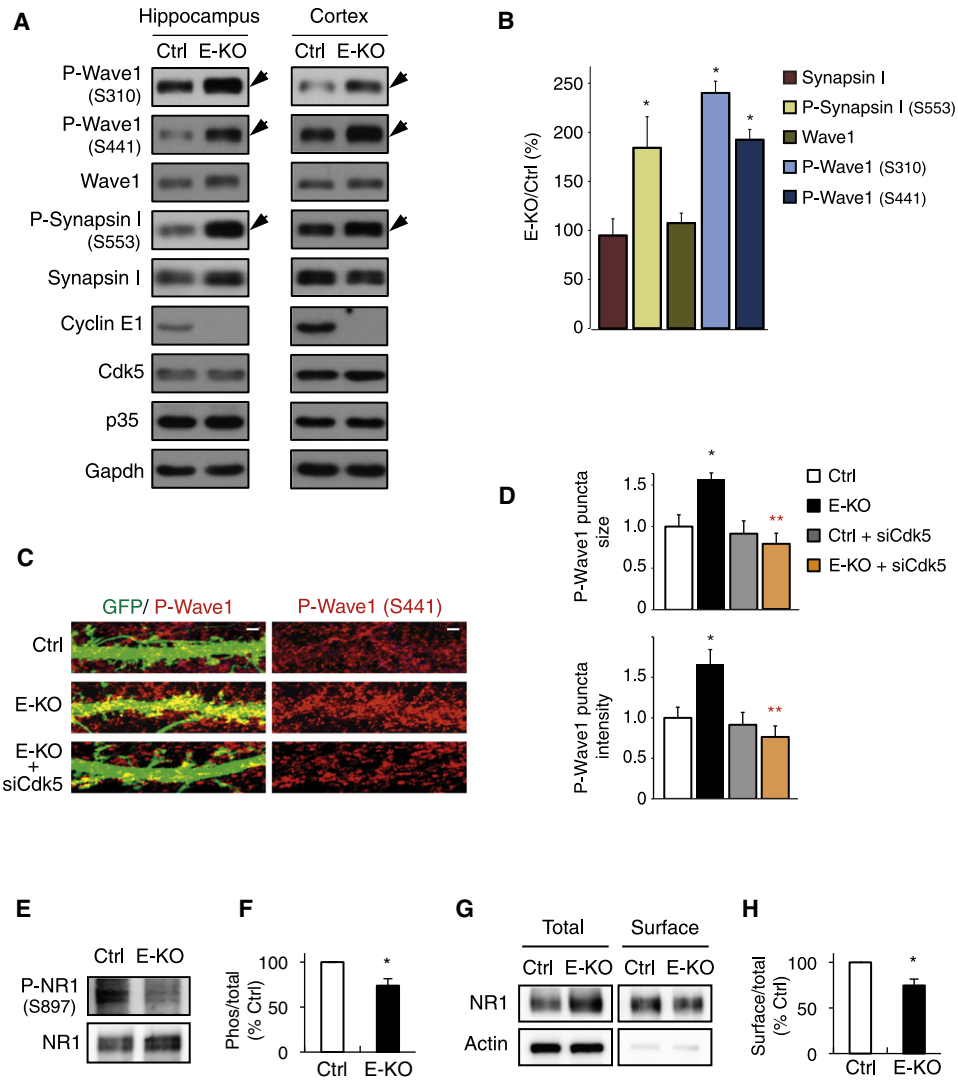

Figure 5. Molecular Analyses of Brains from Adult Conditional *Cyclin E* Knockout Mice

(A) Western blot analysis of hippocampi and cortices dissected from *cyclin E1*$^{flox/flox}$*E2*$^{+/-}$ (Ctrl) and *Nestin-Cre/cyclin E1*$^{flox/flox}$*E2*$^{-/-}$ (E-KO) littermates. Immunoblots were probed with antibodies against total Wave1, total Synapsin I, or antibodies recognizing Cdk5-specific phosphoresidues on Wave1 or Synapsin I.

(B) Adult E-KO (n = 14) and control littermates (n = 14) were analyzed as in (A), using hippocampi and cortices as a source of material. Integrated intensities were calculated by densitometry measurements of immunoblots in ImageJ, and were normalized to averages of tubulin and Gapdh levels. Data are shown as change relative to littermate controls (Ctrl) and represent mean ± SEM. *p < 0.05; Student's t test.

(C) Images of GFP-transfected *cyclin E1*$^{flox/flox}$*E2*$^{+/-}$ (Ctrl), or GFP- and Cre-transfected *cyclin E1*$^{flox/flox}$*E2*$^{-/-}$ (E-KO) hippocampal neurons stained for phospho-Wave1 (S441). Also shown is an image of a *cyclin E1*$^{flox/flox}$*E2*$^{-/-}$ neuron transfected with GFP, Cre, and Cdk5 siRNA (E-KO + siCdk5).

(D) Normalized quantification of size and intensity of phospho-Wave1 puncta in hippocampal neurons, transfected as in (C). Data are normalized to GFP-transfected control and represent mean ± SEM from three independent experiments; total numbers of neurons analyzed, n = 30–60 cells/condition. *p < 0.05 versus Ctrl; red **p < 0.05 versus E-KO; one-way ANOVA with pairwise comparison by Bonferroni post hoc test.

(E) Immunoblot analysis showing phospho-Ser897 (P-NR1) and total levels of NR1 subunit in hippocampi of adult E-KO and control littermates.

(F) Quantification of P-NR1 (ratio of P-NR1 to total NR1) in E-KO (n = 4) and control (n = 4) animals. Data are normalized to Ctrl and represent mean ± SEM. *p < 0.01; Student's t test.

(G) Immunoblot analysis showing total NR1 levels, and cell-surface NR1 levels.

(H) Quantification of NR1 cell-surface levels (ratio of surface to total) in E-KO (n = 4) and control (n = 4) animals. Data are normalized to Ctrl and represent mean ± SEM. *p < 0.01; Student's t test.

See also Figure S5.

Ser310 and Ser441 by Cdk5 was shown to inhibit Wave1 activity (Kim et al., 2006). Wave1 promotes dendritic spine maturation, and its inhibition leads to a decrease in the number of mature dendritic spines. Moreover, Wave1 activity is essential for hippocampal-dependent learning and memory (Soderling et al., 2003).

In addition to this direct inhibition of synaptic proteins, Cdk5 can also negatively regulate the function of glutamate *N*-methyl-D-aspartate (NMDA) receptors (Chergui et al., 2004). Specifically, Cdk5 was shown to inhibit phosphorylation of the NR1 subunit of NMDA receptors, by inhibiting cAMP-dependent protein kinase (PKA), which phosphorylates NR1 on Ser897 (Chergui et al., 2004). Importantly, PKA-mediated phosphorylation of NR1 is required for synaptic and cell surface localization of this NMDA receptor subunit, and therefore for the receptor function (Bird et al., 2005; Crump et al., 2001). Hence, hyperactivation of Cdk5 is predicted to reduce NR1 phosphorylation on Ser897, and consequently to reduce its incorporation into membrane-bound NMDA receptors. Indeed, we observed reduced phosphorylation of NR1 subunit on Ser897, and reduced surface expression of NR1 in *cyclin E* null hippocampi (Figures 5E–5H), consistent with increased Cdk5 activity in *cyclin E* knockout brains, and with the inhibitory role of active Cdk5 on NMDA receptor assembly (Chergui et al., 2004).

Synaptic Defects in Brains of *Cyclin E* Knockout Mice

We next investigated the brains of conditional *cyclin E* knockout-*Nestin-Cre* animals for signs of impaired synapse structure and function. First, we analyzed dendritic spines in hippocampal CA1 pyramidal neurons by Golgi impregnation. Our analyses revealed that the spine length, width and estimated spine volume were reduced in adult *cyclin E* null brains (Figures 6A and 6B and Figures S6A and S6B). Consistent with the above, analyses of transmission electron microscopic images of CA1 stratum radiatum demonstrated a reduced length of postsynaptic densities in *cyclin E* null brains (Figures 6C–6E). Hence, ablation of cyclin E in the brains of conditional *cyclin E* knockout animals led to both molecular (reduced incorporation of NMDA receptor subunit) and ultrastructural synaptic abnormalities.

To substantiate these observations at a functional level, we analyzed spontaneous excitatory postsynaptic currents (sEPSC), which gauge synaptic activity, using acute hippocampal slices. We found that the frequency of sEPSC in CA1 pyramidal neurons was greatly reduced in cyclin E knockout brains (Figures 6F and 6G and Figures S6C–S6E). To evaluate changes in the activity of NMDA receptors, we isolated the NMDA component of sEPSC as described in Supplemental Experimental Procedures. The NMDA component made up 41.5 ± 6.9% (SEM) in control mice, and it was reduced to 27.5 ± 6.5% (SEM) in cyclin E knockouts (Figures S6F and S6G). These observations reveal reduced synaptic transmission, and reduced NMDA-dependent currents in the brains of *cyclin E* knockout animals.

Defective Synaptic Plasticity and Memory Deficits in *Cyclin E* Knockout Mice

The ultrastructural, molecular and electrophysiological synaptic abnormalities seen in *cyclin E* knockout brains suggested that cyclin E-deficient mice might display impaired learning and memory, as these processes critically depend on proper synaptic function. Of note, *Cdk5* knockout mice were shown to display enhanced memory formation, consistent with inhibitory role of Cdk5 in synaptic plasticity (Hawasli et al., 2007). Therefore, we hypothesized that *cyclin E* knockout mice, which showed signs of Cdk5 hyperactivation, might display impaired memory.

Long-term potentiation (LTP) represents an electrophysiological correlate of learning and memory (Cooke and Bliss, 2006). Therefore, we first analyzed LTP in CA1 hippocampal neurons of conditional *cyclin E* knockout-*Nestin-Cre* animals, following theta-burst stimulation of the Schaffer collateral inputs. We observed reduced LTP in *cyclin E* knockouts, revealing an impaired synaptic plasticity upon cyclin E loss (Figure 7A and Figures S7A–S7C). Importantly, LTP in CA1 pyramidal neurons is NMDA receptor-dependent (Tsien et al., 1996), hence its reduction is in agreement with the reduced cell surface expression of an essential NMDA receptor subunit, NR1, found in *cyclin E* null brains (Figures 5E–5H).

To extend these observations to an in vivo setting, we turned to the Morris water maze task. This test is also critically dependent on hippocampal CA1 NMDA receptors function (Tsien et al., 1996), and it measures spatial learning and memory. Importantly, expression of the *Nestin-Cre* transgene was shown to have no effect on its own on performance of mice in this test (Fleischmann et al., 2003; Raivich et al., 2004). Conditional *cyclin E* knockout and control mice were trained to learn the position of a water-submerged platform (Figure S7D), and then the platform was removed to assess the retention of memory for spatial configuration. *Cyclin E* knockout mice showed impaired performance in this test (Figure 7B), revealing spatial memory deficits. We next tested hippocampal- and NMDA receptor-dependent (Bernasconi-Guastalla et al., 1994; Nakazawa et al., 2003) cognitive flexibility by moving the platform to the opposite quadrant, and retraining the animals to find the platform in a new location (reversal learning). *Cyclin E* knockout mice also showed a significant impairment in spatial reversal learning (Figure 7C and Figures S7E and S7F). Collectively, all these observations revealed that cyclin E loss results in impaired synaptic plasticity, decreased memory formation and impaired cognitive flexibility, phenotypes opposite to the ones observed upon Cdk5 ablation. Importantly, the overall behavioral pattern was not perturbed in cyclin E-deficient mice, as evidenced by normal performance of these animals in a battery of control locomotor, sensorimotor and behavioral tests (Figures S7G–S7K).

DISCUSSION

Cyclin E belongs to the core cell cycle machinery, which has been conserved from yeast to humans. The function of this machinery is to drive cell cycle progression. Indeed, many phosphorylation substrates of yeast and mammalian cyclin-Cdk enzymes represent proteins involved in cell division (Hwang and Clurman, 2005; Sherr and Roberts, 2004; Ubersax et al., 2003). Consistent with this notion, analyses of knockout mice lacking particular cyclins or Cdks revealed distinct proliferative deficits in specific compartments (reviewed in Sherr and Roberts, 2004). The relatively narrow, tissue-specific phenotypes of most cyclin- or Cdk-deficient strains underscored the overlapping, redundant functions of individual cyclins and Cdks in driving cell proliferation.

In clear distinction to these proliferative phenotypes, the work presented here revealed unexpectedly that mammalian cyclin E, a cancer-related protein that normally serves to drive cell division, plays a cell cycle-independent and rate-limiting function in terminally differentiated neurons by controlling synapse

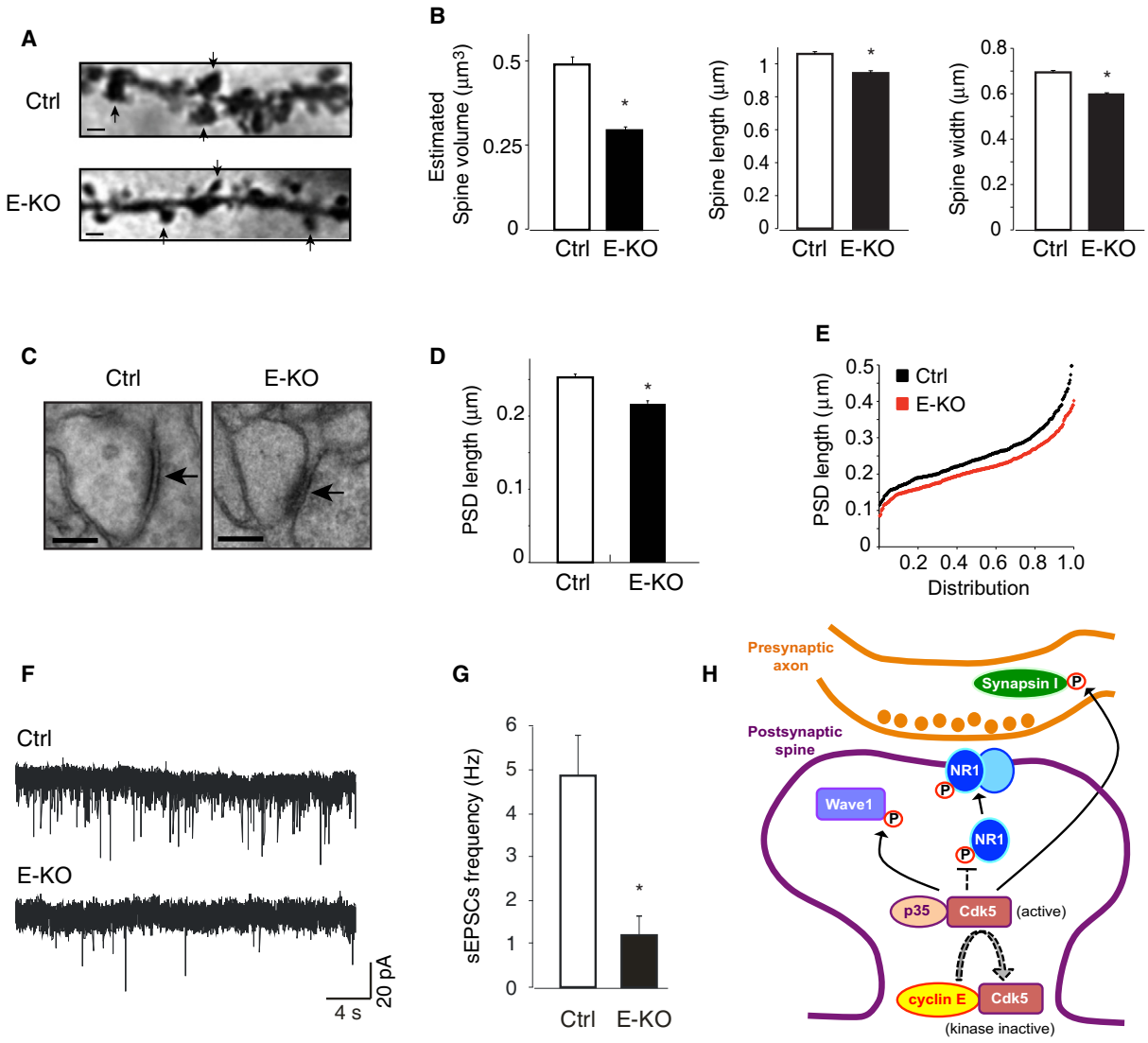

Figure 6. Synaptic and Dendritic Spine Deficiencies in Conditional *Cyclin E* Knockout Mice

(A) Representative images of Golgi-impregnated hippocampal CA1 pyramidal neurons with dendritic spines (arrows). Scale bars represent 1 μm.

(B) Quantification of the length, width, and estimated volume of dendritic spines in Golgi-impregnated hippocampal CA1 pyramidal neurons from adult E-KO and control littermates. Shown are means ± SEM from two E-KO and two control littermates; total numbers of dendritic segments analyzed, n = 19–21 per genotype. Spine volumes represent only estimates, based on the assumption that spines have cylindrical shapes (see Supplemental Experimental Procedures). *$p < 0.05$ versus Ctrl; one-way ANOVA with pairwise comparison by Bonferroni post hoc test.

(C) Representative transmission electron microscopy (EM) images from the hippocampal CA1 stratum radiatum region in adult *Nestin-Cre/cyclin* $E1^{flox/flox}E2^{-/-}$ (E-KO) and cyclin $E1^{flox/flox}E2^{+/-}$ (Ctrl) littermates. Arrows point to excitatory synapses identified by electron-dense postsynaptic densities (PSD). Scale bars represent 100 nm.

(D) Mean PSD length determined by analyses of EM images. Shown are means ± SEM from two E-KO and two control littermates; total numbers of asymmetric excitatory PSDs analyzed, n = 140–180 per genotype. *$p < 0.05$ versus Ctrl; one-way ANOVA with pairwise comparison by Bonferroni post hoc test.

(E) Cumulative frequency distribution of PSD length observed in EM analysis of brains from adult E-KO and control mice, analyzed as in (D). The PSD densities did not differ between E-KO and Ctrl mice (mean ± SEM per 25 μm^2: 13.31 ± 0.60 and 13.49 ± 0.59, respectively).

(F) Representative excitatory postsynaptic current (EPSC) recordings from CA1 pyramidal neurons from *cyclin* $E1^{flox/flox}E2^{+/-}$ (Ctrl) and *Nestin-Cre/cyclin* $E1^{flox/flox}E2^{-/-}$ (E-KO) mice.

(G) Mean frequencies of EPSC from Ctrl and E-KO mice. Values are mean ± SEM. *$p < 0.01$; Student's t test, n = 10 Ctrl and 5 E-KO.

(H) A model how cyclin E controls Cdk5 synaptic function.

See also Figure S6.

formation and function. We found that acute ablation of cyclin E in postmitotic neurons led to a reduced number of synapses and dendritic spines, and resulted in decreased synaptic transmission. To ablate cyclin E in vivo, we used conditional *cyclin E* knockout-*Nestin-Cre* mice. In these animals, deletion of cyclin E occurred during embryonic development, which might

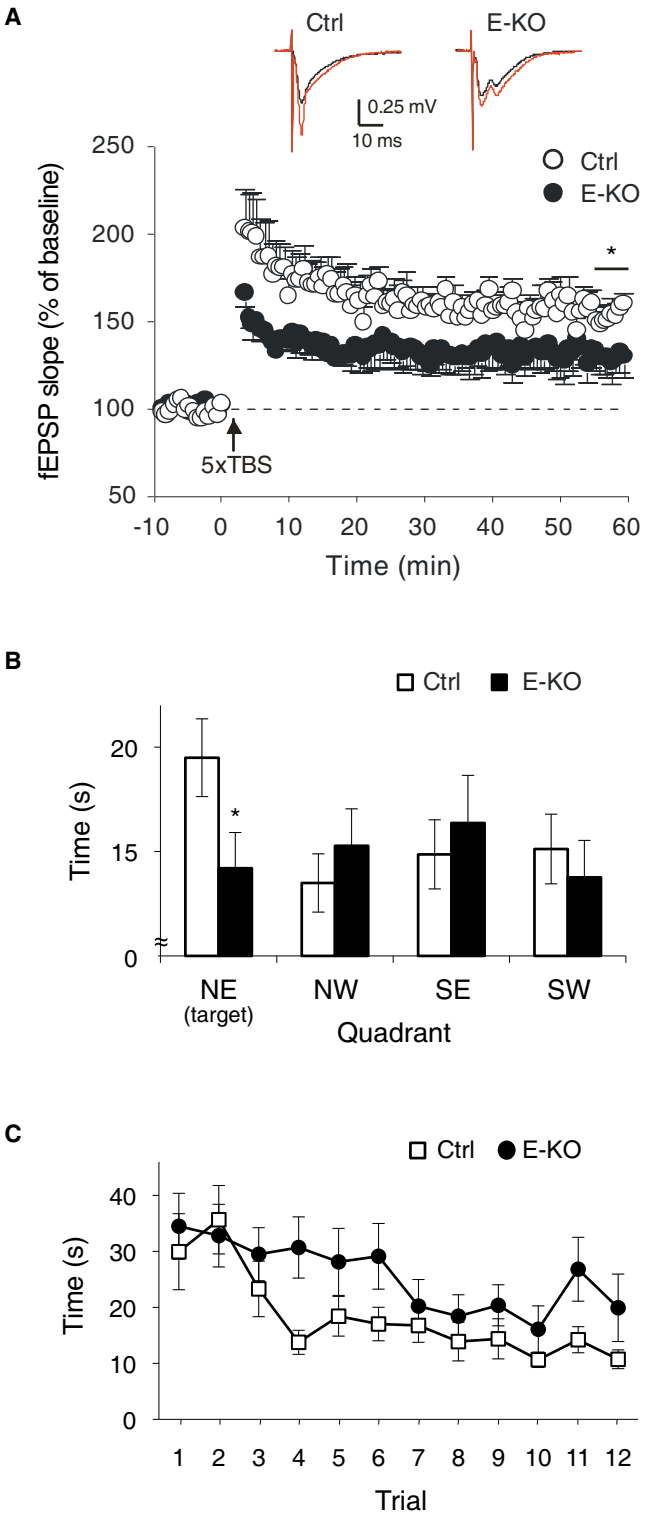

Figure 7. Impaired Synaptic Plasticity and Memory in Conditional *Cyclin E* Knockout Mice

(A) LTP was induced by five theta-burst stimulation trains (5× TBS, arrow) delivered to Schaffer collateral pathway with 30 s interstimulus interval. Values are mean ± SEM. Reduced LTP was observed in *cyclin E* knockouts (Ctrl: 154.6 ± 1.5% of baseline, E-KO: 130.8 ± 1.1% of baseline). *p < 0.001; Student's t test, n = 5 Ctrl and 5 E-KO. Inserts show representative recordings taken during the first (black) and last (red) 5 min of recording.

(B) Morris water maze paradigm. Results of a probe test after several training sessions showing time spent in different quadrants (NE, northeast; NW, northwest; SE, southeast; SW, southwest). In contrast to control mice, E-KO showed no preference to the target quadrant (NE) during the probe test (n = 10 Ctrl and 10 E-KO).

(C) Water maze reversal learning. Escape latencies (time spent prior to finding the platform) were measured during reversal sessions (four trials per day). Data in (B) and (C) represent mean ± SEM. *p < 0.05; Student's t test.

See also Figure S7.

have impacted our analyses of adult cyclin E-deficient brains. However, we verified that ablation of cyclin E did not affect proliferation rates of embryonic brains and did not disturb brain development, as was the case in most other compartments of *cyclin E* null mice (Geng et al., 2003). Moreover analyses of brain-specific *cyclin E* knockout mice revealed very similar defects to the ones observed by us upon acute cyclin E shutdown in postmitotic neurons. In fact, the phenotypes seen in conditional *cyclin E* knockout-*Nestin Cre* mice were milder than those encountered upon acute cyclin E shutdown, a phenomenon seen in other knockouts and ascribed to developmental compensatory mechanisms (Lin et al., 2008).

We propose that cyclin E affects synapse function and memory formation by sequestering Cdk5 into catalytically inactive complexes, thereby affecting the phosphorylation status and function of synaptic proteins (Figure 6H). Hence, cyclin E acts in this setting as a Cdk antagonist, in distinction to the well-described function of cyclins as Cdk activators. Consistent with this model, overexpression of Cdk5 phenocopied acute cyclin E loss, whereas knock-down of Cdk5 restored normal numbers of synapses and dendritic spines in *cyclin E* null neurons. Moreover, we observed hyperphosphorylation of synaptic Cdk5 substrates on Cdk5-specific sites upon acute cyclin E shutdown in vitro, and in the brains of *cyclin E* knockout animals. Hyperactivation of Cdk5 is also expected to indirectly affect other events relevant for learning and memory, such as NR1 subunit localization shown here, but also phosphorylation of CREB on Ser133 by a PKA-dependent pathway (Sindreu et al., 2007). These abnormalities likely collectively contribute to decreased synaptic function and to memory deficits observed in *cyclin E* knockout mice. It should be noted that in addition to its inhibitory function, Cdk5 was also shown to play positive roles in synaptogenesis and synapse function, for example by phosphorylating the CASK protein and by regulating the interaction between CASK and liprin-α (Samuels et al., 2007). It remains to be seen how these steps proceed in the absence of cyclin E.

Further studies will be needed to determine whether ablation of cyclin E results in decreased formation of new synapses and dendritic spines, reduced maintenance of the existing ones, or both. Importantly, active learning has been associated both with formation and maintenance of new dendritic spines in the brains (Xu et al., 2009; Yang et al., 2009). Given the influence of cyclin E in this process, it will be interesting to determine whether the levels of cyclin E in the brain change locally during learning and memory formation. A related question is what pathways control the abundance of cyclin E in terminally differentiated brain cells. In proliferating cells, the initial induction of E-type cyclins is driven at the transcriptional level by E2F

transcription factors, whereas proteolytic degradation of cyclin E is brought about by SCF^{Fbw7} ubiquitin ligase (Hwang and Clurman, 2005). In postmitotic cells the E2Fs are thought to be held in a transcriptionally inactive state by pRB-like "pocket" proteins (Attwooll et al., 2004), therefore it is likely that the proteolytic machinery would be responsible for modulating cyclin E levels.

Of note, the ability of cyclin E to interact with Cdk5 in neurons was also reported by Miyajima et al. (1995), however our current work reveals the functional relationship between these two proteins. To the best of our knowledge, this is the first demonstration of a function for a cyclin protein in the formation of neuronal synaptic circuits and memories.

Cdk5 is considered as an essential regulator of neuronal differentiation, and it acts in a complex with its noncyclin activators p35 or p39. Cdk5-p35/p39 complexes phosphorylate several neuronal proteins, and control a wide range of functions, including synapse formation and plasticity, neuronal migration, axon guidance, membrane transport, and neurite outgrowth (Dhavan and Tsai, 2001). It remains to be seen whether cyclin E affects all these Cdk5 functions, or it only serves to control Cdk5 in its synaptic role.

Another question raised by this work is whether abnormal levels or activity of cyclin E underlie human learning disabilities, cognitive disorders, and other pathological conditions. Indeed, cyclin E is a major target of PARK2, an E3 ubiquitin-ligase, mutations in which are one of the most common cause of early-onset Parkinson's disease. (Staropoli et al., 2003; Lücking et al., 2000). Moreover, Cdk5 has been implicated in several human neurological and neurodegenerative diseases, such as Alzheimer's disease (Cruz and Tsai, 2004; Dhavan and Tsai, 2001), making cyclin E a potential player in these conditions. Interestingly, recent work indicates that reduction of Cdk5 levels can decrease pathological changes and reduce neuronal loss in an Alzheimer's disease mouse model (Piedrahita et al., 2010). These observations suggest an exciting possibility that cyclin E, a protein we demonstrate to bind and inhibit Cdk5, might offer a therapeutic tool for ameliorating this devastating disease.

EXPERIMENTAL PROCEDURES

Generation of Tagged *Cyclin E1* Knock-In Mice

A targeting vector to knock-in a Flag-HA tag at the N terminus of the *cyclin E1* gene was constructed by replacing a start codon in the second exon with DNA sequences encoding an initiation methionine and Flag-HA tag. The targeting vector was electroporated into embryonal stem (ES) cells and homozygous *cyclin* $E1^{Ntag/Ntag}$ animals were obtained using standard procedures (Geng et al., 2003).

Generation of Conditional *Cyclin E* Knockout Mice

Conditional *cyclin E1* gene-targeting construct was assembled by inserting *loxP* sites into ScaI sites in the introns 4 and 11 of the murine *cyclin E1* gene. The gene-targeting construct was electroporated into ES and homozygous *cyclin* $E1^{flox/flox}$ mice were obtained. *Cyclin* $E1^{flox/flox}$ mice were interbred with *cyclin* $E2^{-/-}$ mice (Geng et al., 2003). *Nestin-Cre* animals (Tronche et al., 1999) were from the Jackson Laboratory.

Purification of Cyclin E1-Containing Complexes from Embryonic and Adult Brains and Quantitative Proteomic Analyses

For a single purification, we used pooled 30 brains dissected from 1-month-old mice, or 20 heads dissected from E14.5 embryos. Tissues were homogenized, cyclin E1 and its associated proteins were immunoprecipitated using anti-Flag M2 agarose (Sigma), eluted twice with Flag peptides (Sigma), then immunoprecipitated again with anti-HA antibody (12CA5 ascites fluid, Covance) coupled to protein A Sepharose beads (Amersham). Complexes were eluted from HA beads with 0.1 M glycine (pH 2.5). For LC-MS/MS, purified protein complexes containing at least 200–300 ng of cyclin E1 were used for a single run. LC-MS/MS, data analysis, iTRAQ labeling, and quantitative mass spectrometry are described in Supplemental Experimental Procedures.

Protein Extraction, Immunoblot Analyses, and In Vitro Kinase Assays

These were performed using standard procedures. For the list of antibodies, please see Supplemental Experimental Procedures. For kinase assays, cell lysates were immunoprecipitated with HA beads and incubated at 30°C for 30 min in reaction buffer with 10 μCi [γ^{32}P]-ATP, together with one of the following substrates: pRB (0.5 μg; Santa Cruz), Histone H1 (1 μg; Roche) or GST-Synapsin I (1 μg).

Immunostaining of Brain Sections

Mice were cardiac perfused with PBS and then with paraformaldehyde (4% in PBS). Brains were extracted, postfixed in paraformaldehyde, embedded in tissue freezing medium (Triangle Biomedical Sciences), and frozen. Coronal sections (12 μm) were cut, stained as described in Supplemental Experimental Procedures, mounted with Fluoromount-G (SouthernBiotech), and analyzed using a fluorescent (Nikon E600) or confocal microscope (Leica SP5X).

Hippocampal Neuron Cultures

Dissociated hippocampal neurons were prepared from 16- to 17-day-old mouse embryos. Neurons were maintained in Neurobasal Medium (Invitrogen), supplemented with 2% B27 (Invitrogen), penicillin (100 U/ml), streptomycin (100 mg/ml), and 2 mM glutamine. Neurons were transfected using the Lipofection method (Invitrogen) according to the manufacturer's suggestions. For immunocytochemistry, neurons were fixed in 4% paraformaldehyde/4% sucrose in PBS, incubated with the indicated antibodies (see Supplemental Experimental Procedures) and imaged using a laser scanning Zeiss Pascal microscope.

Organotypic Slice Cultures

Transverse hippocampal slices of 350 μm were prepared from 5- to 7-day-old mice and cultured. Slice cultures were transfected using a Helios Gene Gun (BioRad) at day 7 of culture (day in vitro [DIV]). For each bullet, up to three different plasmids comprising a total of 50 μg of DNA were coated onto 12.5 mg of 1.6 μm gold particles, according to the manufacturer's protocol (BioRad). Slices were fixed at 13 DIV in 2.5% paraformaldehyde and 4% sucrose and processed for immunofluorescence as described above.

Confocal Image Analysis and Quantification

For dissociated neurons, images were obtained using a Zeiss Pascal confocal microscope. On average, a Z stack of five to seven optical sections (0.5 μm/section) was taken for each neuron imaged. Images were collected from 10 to 15 neurons per coverslip, with two coverslips for each condition per experiment. Synapse density, puncta size, and intensity were measured using Metamorph software (Universal Imaging Corporation). Statistical significance was assessed using one-way ANOVA with a Bonferroni post test (Prism-GraphPad Software). For dendritic spine analysis, a Z series projection of proximal apical secondary dendrites was made using 10–50 stacks (0.3 μm/stack), each averaged four times. Statistical significance was assessed using a one-way ANOVA with a Bonferroni post test (Prism-GraphPad Software).

Electrophysiological Analyses of In Vitro Neuronal Cultures

Primary hippocampal neurons were nucleofected with GFP or GFP and Cre after dissection. To record currents from those cells, the whole-cell configuration of the patch-clamp technique was used. Cells were voltage-clamped at an electrode potential of −60 mV. The analysis of mEPSC amplitude and frequency were performed with MiniAnalysis software (Synaptosoft). Currents were recorded using an Axopatch 200B amplifier, low-pass filtered at 2 kHz, digitized at 10 kHz using a Digidata 1320A interface, and acquired using pCLAMP10 software (Molecular Devices) on to the hard drive of a PC for off-line analysis.

Surface Labeling of Brain Slices

Hippocampal slices were prepared with a microslicer (Leica VT1000S) and placed into biotinylation reagent solution of 1 mg/ml NHS-SS-biotin (Pierce). Slices were homogenized and mixed with 40 μl of Streptavidin beads (Pierce). The beads were collected; the bound proteins were analyzed by SDS-PAGE and immunoblotting.

Golgi Impregnation and Analyses of Dendritic Spines

Brains dissected from adult (2- to 3-month-old) male conditional cyclin E knockout-Nestin-Cre and control littermates were stained using FD Rapid Golgi Stain Kit (FD Neuro Technologies). Coronal sections (100 μm) were cut and analyzed using a conventional upright microscope under transmitted light. Using Neurolucida software (MBF Bioscience), CA1 pyramidal neurons were reconstructed and spine densities and sizes were quantified. Both spine length and width were measured using Metamorph software. Statistical significance was assessed using a multifactorial ANOVA with a Bonferroni post test (Prism-GraphPad Software).

Electron Microscopy

Animals were perfused intracardially with 2.5% glutaraldehyde, 2% paraformaldehyde. Tissues were postfixed with 1% osmium tetroxide (OsO4)/1.5% potassium ferrocyanide (KFeCN6) and embedded in TAAB Epon.

Ultrathin sections were stained with lead citrate and examined in a JEOL 1200EX or a TecnaiG^2 Spirit BioTWIN transmission electron microscope. Images were recorded with an AMT 2k CCD camera. PSD length was measured using Metamorph software. Statistical significance was assessed using a multi-factorial ANOVA with a Bonferroni post test (Prism-GraphPad Software).

Electrophysiological Analyses of Acute Hippocampal Slices

Transversal hippocampal brain slices were prepared from 2- to 3-month-old male conditional *cyclin E* knockout-*Nestin-Cre* and control mice. LTP was induced by theta-burst stimulation of Schaffer collaterals repeated five times at 30 s intervals. Whole cell patch-clamp recordings from CA1 neurons were made at holding potential of −70 mV, low-pass filtered at 2 kHz, and sampled at rate of 10 kHz (Molecular Devices). Off-line analysis of excitatory synaptic currents (EPSC) was made using Minianalysis (Synaptosoft) and pClamp (Molecular Devices) software. To isolate the NMDA component of EPSC, recordings were made in magnesium (Mg)-free solution prior and during application of NMDA receptor antagonist, APV (20 μM).

Behavioral Analyses

These were performed on adult 2- to 3-month-old male conditional *cyclin E* knockout-*Nestin-Cre* and control littermates, as described in Supplemental Experimental Procedures.

SUPPLEMENTAL INFORMATION

Supplemental Information includes seven figures, two tables, and Supplemental Experimental Procedures and can be found with this article online at doi:10.1016/j.devcel.2011.08.009.

ACKNOWLEDGMENTS

We thank Drs. R. Bronson, J-S Guan, M. Morabito, G. Corfas, Q. Ma, L-H. Tsai, H. Gardner, M. Ericsson, J. Wang, L. Richey, Y. Haydon, and J.C. Dodart for help and advice, Dr. L. Le Cam for *cyclin E1^{flox}* construct, Y. Kim and P. Greengard for anti-phospho-S310 and -S441 and anti-total Wave1 antibodies, R. Betarbet for anti-phospho-Ser897 NR1 antibody, T. Ryan and P. De Camilli for Synapsin I cDNA. This work was supported by NIH grant R01 CA108950 (to P.S.).

Received: December 31, 2010
Revised: July 25, 2011
Accepted: August 9, 2011
Published online: September 22, 2011

REFERENCES

Attwooll, C., Lazzerini Denchi, E., and Helin, K. (2004). The E2F family: specific functions and overlapping interests. EMBO J. *23*, 4709–4716.

Bernasconi-Guastalla, S., Wolfer, D.P., and Lipp, H.P. (1994). Hippocampal mossy fibers and swimming navigation in mice: correlations with size and left-right asymmetries. Hippocampus *4*, 53–63.

Bird, G.C., Lash, L.L., Han, J.S., Zou, X., Willis, W.D., and Neugebauer, V. (2005). Protein kinase A-dependent enhanced NMDA receptor function in pain-related synaptic plasticity in rat amygdala neurones. J. Physiol. *564*, 907–921.

Chergui, K., Svenningsson, P., and Greengard, P. (2004). Cyclin-dependent kinase 5 regulates dopaminergic and glutamatergic transmission in the striatum. Proc. Natl. Acad. Sci. USA *101*, 2191–2196.

Cooke, S.F., and Bliss, T.V. (2006). Plasticity in the human central nervous system. Brain *129*, 1659–1673.

Crump, F.T., Dillman, K.S., and Craig, A.M. (2001). cAMP-dependent protein kinase mediates activity-regulated synaptic targeting of NMDA receptors. J. Neurosci. *21*, 5079–5088.

Cruz, J.C., and Tsai, L.H. (2004). Cdk5 deregulation in the pathogenesis of Alzheimer's disease. Trends Mol. Med. *10*, 452–458.

Dhavan, R., and Tsai, L.H. (2001). A decade of CDK5. Nat. Rev. Mol. Cell Biol. *2*, 749–759.

Fleischmann, A., Hvalby, O., Jensen, V., Strekalova, T., Zacher, C., Layer, L.E., Kvello, A., Reschke, M., Spanagel, R., Sprengel, R., et al. (2003). Impaired long-term memory and NR2A-type NMDA receptor-dependent synaptic plasticity in mice lacking c-Fos in the CNS. J. Neurosci. *23*, 9116–9122.

Geng, Y., Yu, Q., Whoriskey, W., Dick, F., Tsai, K.Y., Ford, H.L., Biswas, D.K., Pardee, A.B., Amati, B., Jacks, T., et al. (2001). Expression of cyclins E1 and E2 during mouse development and in neoplasia. Proc. Natl. Acad. Sci. USA *98*, 13138–13143.

Geng, Y., Yu, Q., Sicinska, E., Das, M., Schneider, J.E., Bhattacharya, S., Rideout, W.M., Bronson, R.T., Gardner, H., and Sicinski, P. (2003). Cyclin E ablation in the mouse. Cell *114*, 431–443.

Graus-Porta, D., Blaess, S., Senften, M., Littlewood-Evans, A., Damsky, C., Huang, Z., Orban, P., Klein, R., Schittny, J.C., and Müller, U. (2001). Beta1-class integrins regulate the development of laminae and folia in the cerebral and cerebellar cortex. Neuron *31*, 367–379.

Gudas, J.M., Payton, M., Thukral, S., Chen, E., Bass, M., Robinson, M.O., and Coats, S. (1999). Cyclin E2, a novel G1 cyclin that binds Cdk2 and is aberrantly expressed in human cancers. Mol. Cell. Biol. *19*, 612–622.

Hawasli, A.H., Benavides, D.R., Nguyen, C., Kansy, J.W., Hayashi, K., Chambon, P., Greengard, P., Powell, C.M., Cooper, D.C., and Bibb, J.A. (2007). Cyclin-dependent kinase 5 governs learning and synaptic plasticity via control of NMDAR degradation. Nat. Neurosci. *10*, 880–886.

Hwang, H.C., and Clurman, B.E. (2005). Cyclin E in normal and neoplastic cell cycles. Oncogene *24*, 2776–2786.

Ikeda, Y., Matsunaga, Y., Takiguchi, M., and Ikeda, M.A. (2011). Expression of cyclin E in postmitotic neurons during development and in the adult mouse brain. Gene Expr. Patterns *11*, 64–71.

Kim, S.H., and Ryan, T.A. (2010). CDK5 serves as a major control point in neurotransmitter release. Neuron *67*, 797–809.

Kim, Y., Sung, J.Y., Ceglia, I., Lee, K.W., Ahn, J.H., Halford, J.M., Kim, A.M., Kwak, S.P., Park, J.B., Ho Ryu, S., et al. (2006). Phosphorylation of WAVE1 regulates actin polymerization and dendritic spine morphology. Nature *442*, 814–817.

Koff, A., Cross, F., Fisher, A., Schumacher, J., Leguellec, K., Philippe, M., and Roberts, J.M. (1991). Human cyclin E, a new cyclin that interacts with two members of the CDC2 gene family. Cell *66*, 1217–1228.

Lauper, N., Beck, A.R., Cariou, S., Richman, L., Hofmann, K., Reith, W., Slingerland, J.M., and Amati, B. (1998). Cyclin E2: a novel CDK2 partner in the late G1 and S phases of the mammalian cell cycle. Oncogene *17*, 2637–2643.

Lew, D.J., Dulić, V., and Reed, S.I. (1991). Isolation of three novel human cyclins by rescue of G1 cyclin (Cln) function in yeast. Cell *66*, 1197–1206.

Lew, J., Huang, Q.Q., Qi, Z., Winkfein, R.J., Aebersold, R., Hunt, T., and Wang, J.H. (1994). A brain-specific activator of cyclin-dependent kinase 5. Nature *371*, 423–426.

Lin, Y., Bloodgood, B.L., Hauser, J.L., Lapan, A.D., Koon, A.C., Kim, T.K., Hu, L.S., Malik, A.N., and Greenberg, M.E. (2008). Activity-dependent regulation of inhibitory synapse development by Npas4. Nature *455*, 1198–1204.

Lücking, C.B., Dürr, A., Bonifati, V., Vaughan, J., De Michele, G., Gasser, T., Harhangi, B.S., Meco, G., Denèfle, P., Wood, N.W., et al; French Parkinson's Disease Genetics Study Group; European Consortium on Genetic Susceptibility in Parkinson's Disease. (2000). Association between early-onset Parkinson's disease and mutations in the parkin gene. N. Engl. J. Med. *342*, 1560–1567.

Malumbres, M., and Barbacid, M. (2009). Cell cycle, CDKs and cancer: a changing paradigm. Nat. Rev. Cancer *9*, 153–166.

Matsubara, M., Kusubata, M., Ishiguro, K., Uchida, T., Titani, K., and Taniguchi, H. (1996). Site-specific phosphorylation of synapsin I by mitogen-activated protein kinase and Cdk5 and its effects on physiological functions. J. Biol. Chem. *271*, 21108–21113.

Miyajima, M., Nornes, H.O., and Neuman, T. (1995). Cyclin E is expressed in neurons and forms complexes with cdk5. Neuroreport *6*, 1130–1132.

Morabito, M.A., Sheng, M., and Tsai, L.H. (2004). Cyclin-dependent kinase 5 phosphorylates the N-terminal domain of the postsynaptic density protein PSD-95 in neurons. J. Neurosci. *24*, 865–876.

Nakazawa, K., Sun, L.D., Quirk, M.C., Rondi-Reig, L., Wilson, M.A., and Tonegawa, S. (2003). Hippocampal CA3 NMDA receptors are crucial for memory acquisition of one-time experience. Neuron *38*, 305–315.

Nikolic, M., Dudek, H., Kwon, Y.T., Ramos, Y.F., and Tsai, L.H. (1996). The cdk5/p35 kinase is essential for neurite outgrowth during neuronal differentiation. Genes Dev. *10*, 816–825.

Ohtsubo, M., Theodoras, A.M., Schumacher, J., Roberts, J.M., and Pagano, M. (1995). Human cyclin E, a nuclear protein essential for the G1-to-S phase transition. Mol. Cell. Biol. *15*, 2612–2624.

Parisi, T., Beck, A.R., Rougier, N., McNeil, T., Lucian, L., Werb, Z., and Amati, B. (2003). Cyclins E1 and E2 are required for endoreplication in placental trophoblast giant cells. EMBO J. *22*, 4794–4803.

Piedrahita, D., Hernández, I., López-Tobón, A., Fedorov, D., Obara, B., Manjunath, B.S., Boudreau, R.L., Davidson, B., Laferla, F., Gallego-Gómez, J.C., et al. (2010). Silencing of CDK5 reduces neurofibrillary tangles in transgenic alzheimer's mice. J. Neurosci. *30*, 13966–13976.

Raivich, G., Bohatschek, M., Da Costa, C., Iwata, O., Galiano, M., Hristova, M., Nateri, A.S., Makwana, M., Riera-Sans, L., Wolfer, D.P., et al. (2004). The AP-1 transcription factor c-Jun is required for efficient axonal regeneration. Neuron *43*, 57–67.

Ross, P.L., Huang, Y.N., Marchese, J.N., Williamson, B., Parker, K., Hattan, S., Khainovski, N., Pillai, S., Dey, S., Daniels, S., et al. (2004). Multiplexed protein quantitation in Saccharomyces cerevisiae using amine-reactive isobaric tagging reagents. Mol. Cell. Proteomics *3*, 1154–1169.

Samuels, B.A., Hsueh, Y.P., Shu, T., Liang, H., Tseng, H.C., Hong, C.J., Su, S.C., Volker, J., Neve, R.L., Yue, D.T., and Tsai, L.H. (2007). Cdk5 promotes synaptogenesis by regulating the subcellular distribution of the MAGUK family member CASK. Neuron *56*, 823–837.

Sherr, C.J., and Roberts, J.M. (2004). Living with or without cyclins and cyclin-dependent kinases. Genes Dev. *18*, 2699–2711.

Sindreu, C.B., Scheiner, Z.S., and Storm, D.R. (2007). Ca2+ -stimulated adenylyl cyclases regulate ERK-dependent activation of MSK1 during fear conditioning. Neuron *53*, 79–89.

Soderling, S.H., Langeberg, L.K., Soderling, J.A., Davee, S.M., Simerly, R., Raber, J., and Scott, J.D. (2003). Loss of WAVE-1 causes sensorimotor retardation and reduced learning and memory in mice. Proc. Natl. Acad. Sci. USA *100*, 1723–1728.

Staropoli, J.F., McDermott, C., Martinat, C., Schulman, B., Demireva, E., and Abeliovich, A. (2003). Parkin is a component of an SCF-like ubiquitin ligase complex and protects postmitotic neurons from kainate excitotoxicity. Neuron *37*, 735–749.

Tarricone, C., Dhavan, R., Peng, J., Areces, L.B., Tsai, L.H., and Musacchio, A. (2001). Structure and regulation of the CDK5-p25(nck5a) complex. Mol. Cell *8*, 657–669.

Tronche, F., Kellendonk, C., Kretz, O., Gass, P., Anlag, K., Orban, P.C., Bock, R., Klein, R., and Schütz, G. (1999). Disruption of the glucocorticoid receptor gene in the nervous system results in reduced anxiety. Nat. Genet. *23*, 99–103.

Tsai, L.H., Takahashi, T., Caviness, V.S., Jr., and Harlow, E. (1993). Activity and expression pattern of cyclin-dependent kinase 5 in the embryonic mouse nervous system. Development *119*, 1029–1040.

Tsai, L.H., Delalle, I., Caviness, V.S., Jr., Chae, T., and Harlow, E. (1994). p35 is a neural-specific regulatory subunit of cyclin-dependent kinase 5. Nature *371*, 419–423.

Tsien, J.Z., Huerta, P.T., and Tonegawa, S. (1996). The essential role of hippocampal CA1 NMDA receptor-dependent synaptic plasticity in spatial memory. Cell *87*, 1327–1338.

Ubersax, J.A., Woodbury, E.L., Quang, P.N., Paraz, M., Blethrow, J.D., Shah, K., Shokat, K.M., and Morgan, D.O. (2003). Targets of the cyclin-dependent kinase Cdk1. Nature *425*, 859–864.

Xu, T., Yu, X., Perlik, A.J., Tobin, W.F., Zweig, J.A., Tennant, K., Jones, T., and Zuo, Y. (2009). Rapid formation and selective stabilization of synapses for enduring motor memories. Nature *462*, 915–919.

Yang, G., Pan, F., and Gan, W.B. (2009). Stably maintained dendritic spines are associated with lifelong memories. Nature *462*, 920–924.

Zariwala, M., Liu, J., and Xiong, Y. (1998). Cyclin E2, a novel human G1 cyclin and activating partner of CDK2 and CDK3, is induced by viral oncoproteins. Oncogene *17*, 2787–2798.